OPEN

Virtual Intravascular Endoscopy Visualization of Calcified Coronary Plaques

A Novel Approach of Identifying Plaque Features for More Accurate Assessment of Coronary Lumen Stenosis

Lei Xu, MD and Zhonghua Sun, PhD

Abstract: This study was conducted to investigate the feasibility of using 3D virtual intravascular endoscopy (VIE) as a novel approach for characterization of calcified coronary plaques with the aim of differentiating superficial from deep calcified plaques, thus improving assessment of coronary stenosis.

A total of 61 patients with suspected coronary artery disease were included in the study. Minimal lumen diameter (MLD) was measured and compared between coronary CT angiography (CCTA) (≥64-slice) and invasive coronary angiography (ICA) with regard to the measurement bias, whereas VIE findings were correlated with CCTA with respect to the diagnostic performance of coronary stenosis and the area under the curve (AUC) by receiver-operating characteristic curve analysis (ROC).

In all 3 coronary arteries, the CCTA consistently underestimated the MLD relative to the ICA ($P < 0.001$). On a per-vessel assessment, the sensitivity, specificity, positive predictive value, and negative predictive value and 95% confidence interval (CI) were 94% (95% CI: 61%, 100%), 27% (95% CI: 18%, 38%), 33% (95% CI: 23%, 43%), and 92% (95% CI: 74%, 99%) for CCTA, and 100% (95% CI: 89%, 100%), 85% (95% CI: 75%, 92%), 71% (95% CI: 56%, 84%), and 100% (95% CI: 95%, 100%) for VIE, respectively. The AUC by ROC analysis for VIE demonstrated significant improvement in analysis of left anterior descending calcified plaques compared with CCTA (0.99 vs 0.60, $P < 0.001$), with better performance in the left circumflex and right coronary arteries (0.98 vs 0.84 and 0.77 vs 0.77, respectively; $P = 0.07$ and $P = 0.96$, respectively). There are no significant differences between 64-, 128-, and 640-slice CCTA and VIE in terms of sensitivity, specificity, positive and negative predictive value in the diagnosis of coronary stenosis.

This study shows the feasibility of using VIE for characterizing morphological features of calcified plaques, therefore, significantly improving assessment of coronary stenosis.

Editor: Rosa Sicari.
Received: March 4, 2015; revised: March 30, 2015; accepted: April 1, 2015.
From the Department of Radiology, Beijing Anzhen Hospital, Capital Medical University, Beijing, China (LX); and Discipline of Medical Radiation Sciences, School of Science, Curtin University, Perth, Western Australia, Australia (ZS).
Correspondence: Professor Zhonghua Sun, Discipline of Medical Radiation Sciences, School of Science, Curtin University, GPO Box, U1987, Perth, Western Australia, Australia (e-mail: z.sun@curtin.edu.au).
This work has been supported by research grant for Excellent Talents from Beijing city (2011D003034000030), grant from Natural Science Foundation of China (grant 81271542), and grant for High Levels of Health Technical Personnel in Beijing City Health System (2013–3–011).
The authors report no conflicts of interest in this study.

ISSN: 0025-7974
DOI: 10.1097/MD.0000000000000805

(*Medicine* 94(17):e805)

Abbreviations: AUC = area under the curve, CAD = coronary artery disease, CCTA = coronary computed tomography angiography, CI = confidence interval, DICOM = digital imaging and communications in medicine, HU = Hounsfield unit, ICA = invasive coronary angiography, IVUS = intravascular ultrasound, LAD = left anterior descending, LCx = left circumflex, MLD = minimal lumen diameter, NPV = negative predictive value, OCT = optical coherence tomography, PCI = percutaneous coronary intervention, PPV = positive predictive value, RCA = right coronary artery, ROC = receiver-operating characteristic, VIE = virtual intravascular endoscopy.

INTRODUCTION

Coronary CT angiography (CCTA) is a well-established less-invasive imaging modality for the diagnosis of coronary artery disease (CAD) and its diagnostic value has been significantly augmented due to rapid improvements in CT scanning techniques.[1–5] Despite the very high negative predictive value of CCTA, the diagnostic performance of CCTA is affected by the presence of high calcification in the coronary artery wall, which results in blooming artifacts associated with radiodense calcium deposits within the plaques.[6–8] The negative impact of heavy calcification or severely calcified plaques on the diagnostic specificity is due to overestimation of coronary lumen stenosis, leading to high false-positive findings on CCTA.[9–11] It has been reported that the specificity of CCTA was significantly reduced in patients with high calcification or calcium score in the coronary artery when compared with those with low or no calcification.[6,7] Therefore, high coronary calcification presents a challenge to the diagnostic value of CCTA as patients with severely calcified plaques cannot be reliably assessed with CCTA.

We hypothesized that superficial calcified plaques may easily cause significant stenosis with irregular appearance than deep calcified plaques, which is consistent with findings observed on invasive coronary angiography (ICA), whereas deep calcified plaques may lead to false-positive results, with normal or insignificant stenosis on ICA. The superficial calcified plaques are defined as those arising from the intima of coronary wall, whereas the deep calcified plaques are referred to those originating from the media or adventitia. Our hypothesis is based on previous studies suggesting that calcified plaques may be stabilized, as they rarely cause acute coronary syndromes.[12–14] However, superficial calcified plaques, especially those which are close to the luminal surface, can protrude through and rupture the fibrous cap, resulting in thrombus

formation and acute coronary syndromes.[15] Therefore, from a clinical perspective, identification of calcified plaque features in relation to the coronary wall plays an important role in determining the coronary stenosis and prediction of cardiac events.

Identification of plaque origin is very important for percutaneous coronary intervention (PCI) with rotational atherectomy for severely calcified plaques.[16] If calcified plaques originate from intima (or superficial calcified plaques), PCI procedure could be more difficult and challenging, as severely calcified plaques respond poorly to balloon angioplasty, resulting in incomplete and asymmetrical stent expansion, whereas deep calcified plaques (plaques arising from adventitia) may not be affected by the balloon expansion.[17] Rotational atherectomy may have a role in treating these heavily superficial calcified lesions.[18,19] The less-invasive approach to identify the morphological features of calcified plaques is through 3D virtual intravascular endoscopy (VIE), which has been shown to provide additional information of the coronary wall and plaques.[20–22] Identification of intraluminal appearances of calcified plaques is considered to allow more accurate assessment of coronary stenosis by detecting superficial and deep calcified plaques. Thus, the purpose of this study is to investigate the feasibility of using 3D VIE as a novel approach to differentiate superficial from deep calcified plaques, and determine the accuracy of assessing coronary lumen stenosis when compared with ICA.

TABLE 1. Patient Characteristics (n = 61)

Characteristics	Value
Age, years, mean ± SD	61.2 ± 9.6
Sex (n)	
Men	46 (75%)
Women	15 (25%)
Coronary risk factors (n)	
Hypertension	55 (90%)
Diabetes	22 (36%)
Smoking	50 (82%)
Hyperlipidemia	50 (82%)
Family history	20 (30%)
CCTA HR, beats/min	
Mean ± SD	63.3 ± 7.6
CCTA calcified plaque distribution 1-vessel disease	
LAD	61 (52%)
LCx	23 (20%)
RCA	33 (28%)
2-Vessel disease	25 (21%)
3-Vessel disease	17 (14%)

CCTA = coronary CT angiography, HR = heart rate, LAD = left anterior descending, LCx = left circumflex, RCA = right coronary artery.

METHODS

Patient Data

Between March and August 2014, 161 patients who underwent CCTA examinations were retrospectively reviewed. Our inclusion criteria were patients with suspected CAD having calcified plaques detected on CCTA, whereas ICA was performed as the gold standard technique to confirm the diagnosis. The exclusion criteria were: non-calcified plaques or mixed plaques as observed on CCTA, contraindications for iodinated contrast media, history of coronary stenting or bypass surgery, renal dysfunction or renal failure, and intolerance to beta-blockers. One hundred patients were excluded due to the following reasons: non-calcified or mixed plaques on coronary arteries (n = 35), no ICA available for comparison (n = 60), and coronary stenting (n = 5). Therefore, 61 patients were eligible for inclusion in this study, and patient characteristics are shown in Table 1.

The institutional review board approval was waived in this study since these patients were referred for CCTA scans as a routine procedure for clinical diagnosis. Patients' details were de-identified in all of the images; thus, no informed consent was obtained from patients.

CCTA Scanning Protocol

All patients underwent ≥64-slice CCTA (Somatom Definition and Definition Flash, Siemens Healthcare, Forchheim, Germany; Toshiba Aquilion ONE, Toshiba, Otawara, Japan), including 24 patients (39%) for 64-slice CT, 21 patients (34%) for 128-slice CT, and 16 patients (26%) for 640-slice CT, respectively. The scanning protocols for these CT scanners were as follows: detector collimation $2 \times 32 \times 0.6$ mm/$2 \times 64 \times 0.6$ mm, gantry rotation of 0.33/0.28 s, with a tube voltage of 100 to 120 kVp depending on body mass index and tube current ranging from 345 to 420 mAs/rot and 330 to 450 mAs/rot with retrospective ECG-gating for the 64-slice and 128-slice CT, respectively; detector collimation 320×0.5 mm, gantry rotation of 0.35 s, with a tube voltage of 100 to 120 kVp depending on body mass index and automatic tube current modulation with prospective ECG-gating for the 640-slice CT. Beta-blockers were administered in patients with heart rate >65 bpm (beats per minute) for 640-slice CT scanning and in patients with heart rate >80 bpm for 64- and 128-slice CT scanning.

In all examinations, non-ionic contrast medium Iopromide at 370 mg/mL (Iopromide 370, Bayer Schering Pharma, Berlin, Germany) was delivered using a dual-head power injector. The scan start time was determined with use of bolus tracking technique with a CT attenuation of 120 HU as the triggering threshold in the ascending aorta to initiate the scan. Sixty to 75-mL contrast medium was injected at an injection rate of 4.5 to 5.5 mL/s in the 120-kVp protocol, and 50 to 65-mL contrast medium at an injection rate of 4 to 4.5 mL/s in the 100-kVp protocol. All injections were followed by a saline flush of 30 mL. ECG tube current modulation was used with full tube current from 30% to 75% of the R-R interval. Pitch varied from 0.2 to 0.4 depending on the heart rate for 64- and 128-slice CT protocols. Images were reconstructed with a slice thickness of 0.6 to 0.75 mm and a reconstruction interval of 0.5 to 0.6 mm for 64- and 128-slice CT, 0.5 mm and interval of 0.25 mm for 640-slice CT, respectively.

ICA

ICA was performed by femoral or radial approach. The minimal lumen diameter (MLD) was measured in projections showing the most severe narrowing of 3 main coronary arteries (left anterior descending [LAD], left circumflex [LCx], and right coronary artery [RCA]) by a radiologist with >15 years of experience in cardiac imaging. The MLD was measured 3 times at each coronary lesion, and the mean values were used to avoid intraobserver disagreement. The degree of coronary lumen stenosis was classified into: no stenosis, minimal, or mild

stenosis (<50%), moderate stenosis (50%–70%), and severe stenosis (>70%).

CCTA Measurements of MLD

The MLD was measured on multiplanar/curved planar reformatted images in the views showing the greatest degree of stenosis in 3 main coronary arteries, LAD, LCx, and RCA. Measurements were performed by 2 observers (with >7 and 10 years of experience in cardiac CT imaging, respectively) who were blinded to the results of ICA. Any discrepancy between the observers was resolved by consensus. The interval of MLD measurements in CCTA and ICA was 2 weeks. Similarly, the MLD was measured 3 times at each coronary lesion, and the mean values were used to avoid intraobserver disagreement. Figure 1 shows the landmarks that were used to perform measurement of MLD on both CCTA and ICA images.

Generation of VIE Images for Visualization of Coronary Lumen and Plaques

CT volume data were converted from original DICOM (digital imaging and communications in medicine) images, which were transferred to a separate workstation equipped with Analyze V 11.0 (AnalyzeDirect, Inc, Lexana, KS) for image post-processing and generation of 3D VIE images. Post-processing of CT data was performed with a CT number thresholding technique, which was described before.[20–23] In summary, generation of VIE images of coronary plaques and coronary lumen depends on the selection of appropriate CT threshold, which is determined by measuring the CT attenuation at the coronary arteries according to our previous experience.[20–22] An upper CT threshold of 250 to 300 HU was applied to remove the contrast-enhanced blood from the coronary artery for optimal demonstration of intraluminal views of coronary wall and plaque. VIE images were generated by an observer with >15 years of experience in 3D VIE imaging of cardiovascular disease. Figure 2 is an example of VIE visualization of left coronary ostium and coronary plaque with upper CT threshold of 250 HU applied to generate intraluminal views. As shown in the figure, orthogonal views (coronal and sagittal reformations) are also used to check the exact location of the plaque in relation to the coronary artery.

Our previous studies have shown that VIE visualization demonstrates intraluminal appearances of coronary wall and plaque, which can be characterized into the following categories[20,21]: coronary wall is presented as either smooth or irregular appearances; coronary plaque is shown as either protrusion into the coronary lumen with regular configuration, or protrusion with irregular shape, or irregular intraluminal appearances with resultant coronary stenosis or occlusion. Our hypothesis in this study is that due to its uniqueness of providing intraluminal views, VIE could serve as a potential visualization tool to allow more accurate assessment of coronary lumen stenosis by identifying the morphological features of calcified plaques in terms of superficial and deep types, thus, overcoming the limitations of conventional 2D and 3D visualizations that are commonly encountered in the diagnostic evaluation of CAD. Significant coronary artery disease was determined with ≥50% lumen stenosis as assessed on CCTA, ICA, and VIE measurements.

Statistical Analysis

All data were entered into SPSS 21.0 (SPSS Inc, Chicago, IL) for statistical analysis. Continuous variables were expressed

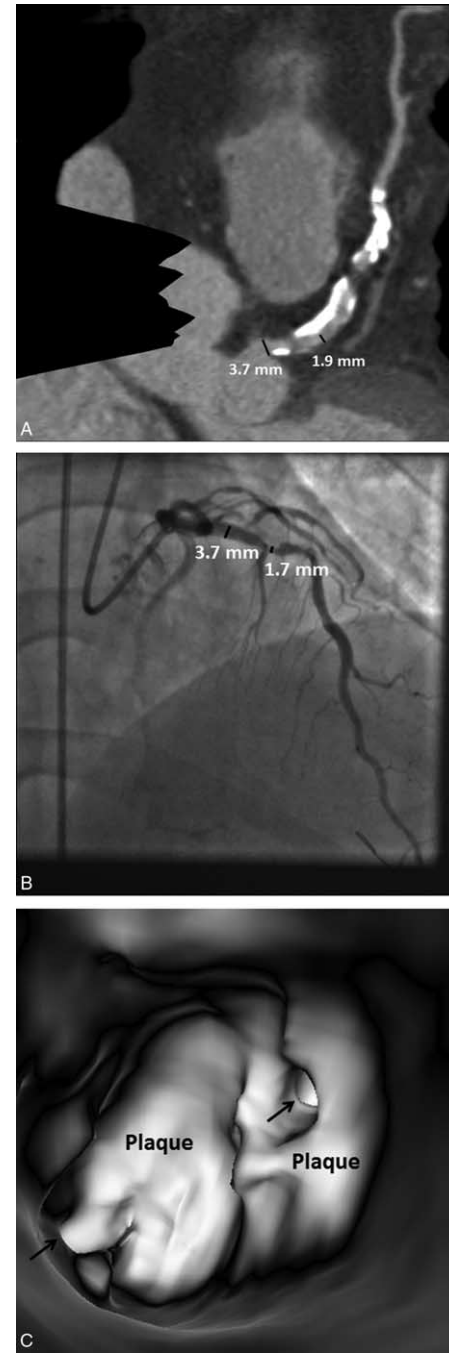

FIGURE 1. Landmarks for measurement of MLD at the LAD coronary artery. (A) MLD was measured 1.9 mm on curved planar reformatted CCTA image, with the reference normal diameter of LAD measured 3.7 mm. (B) The MLD was measured 1.7 mm on ICA with the reference normal diameter of LAD being 3.7 mm. (C) Significant coronary lumen stenosis was observed on virtual intravascular endoscopy due to presence of superficial calcified plaques, which protrude into the lumen, resulting in lumen stenosis. Arrows refer to the residual patent coronary lumen. Please note that at the mid LAD severely calcified plaques result in lumen occlusion (false positive) on CCTA, but this was confirmed to moderate stenosis on ICA as shown in Fig B. CCTA = coronary CT angiography, ICA = invasive coronary angiography, LAD = left anterior descending, MLD = minimal lumen diameter.

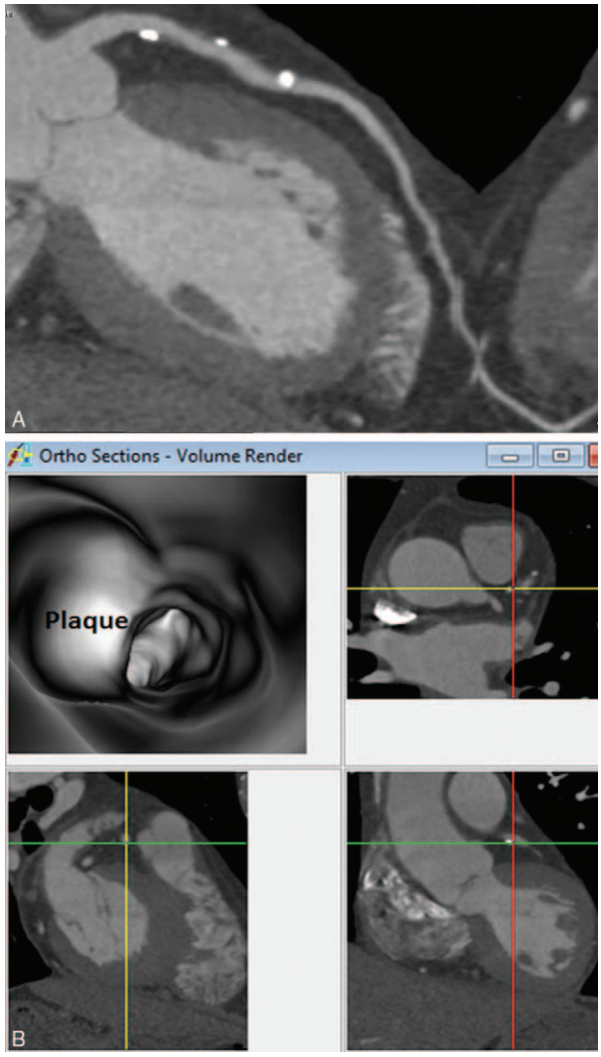

FIGURE 2. (A) Curved planar reformatted coronary CT angiography shows multiple calcified plaques at the left anterior descending. (B) VIE reveals smooth intraluminal appearance of the plaque with no significant lumen stenosis when an upper threshold of 250 HU was applied (top left image). Arrows refer to the left anterior descending coronary ostium. Orthogonal views (top right and bottom row images) are used to verify the plaque location on VIE. VIE = virtual intravascular endoscopy.

as mean ± standard deviation. All variables input to *t* test procedures were first examined for normality with the Kolmogorov–Smirnov test. The 3 arrays of CCTA-ICA differences tested satisfactorily for normality via the Kolmogorov-Smirnov test. Sensitivity, specificity, positive predictive value (PPV), and negative predictive value (NPV) for the detection of significant stenosis on CCTA and VIE were calculated for individual coronary branches and all 3 coronary vessels. Receiver-operating characteristic (ROC) curve analysis was used to assess the diagnostic performance of VIE in the detection of coronary stenosis compared with CCTA by ICA as the gold standard. The area under the ROC curves (AUC) was compared between these 2 methods.

Bland–Altman plot analysis was done to estimate the mean difference in MLD measurements between CCTA and ICA. This provides a visual indication of how the measurement bias varies in the assessment of coronary lumen stenosis due to presence of calcified plaques. A Student *t* test was used to determine whether there is any significant difference between 64-, 128-, and 640-slice CCTA and VIE in the diagnostic assessment of coronary stenosis. A P value of <0.05 was considered statistically significant.

RESULTS

Calcified plaques were found in all of the LAD arteries, whereas plaques were present in 33 RCA and 23 LCx branches, respectively. Calcified plaques were detected in 117 coronary vessels, of which 32 (27%) were confirmed by ICA to be significant stenosis (>50%). No coronary occlusion was found in these patients.

We randomly selected 20 cases (60 vessels) for interobserver variability and the comparison of measurements between CCTA and ICA. The experienced readers blindly measured MLD on both imaging techniques, with high correlation achieved between MLD values performed by 2 observers ($r = 0.954$, $P < 0.001$).

Overall, the MLD measured on CCTA was underestimated in most of the cases, with 96%, 91%, and 88% observed in the lesions in LAD, LCx and RCA, respectively. The Bland–Altman plots seen at Figure 3 show a significant negative bias for the MLD measurements from the zero bias line in comparison with the ICA measurements. So MLD measurements at all 3 coronary arteries exhibited statistically significant evidence of bias ($P < 0.001$). In all 3 sites, the mean bias was negative, indicating that the CCTA method consistently underestimated the MLD relative to the ICA.

3D VIE was successfully generated in all patients with clear demonstration of intraluminal appearances of coronary wall and plaque. Results showed a direct correlation between the plaque type as observed on VIE and corresponding coronary lumen change and degree of lumen stenosis. Table 2 shows the relationship between plaque morphological features and degree of coronary stenosis as assessed on CCTA, ICA, and VIE, as well as corresponding VIE appearances in the 3 coronary arteries. Most of the deep calcified plaques (>80%) as shown on VIE were found to demonstrate no significant stenosis as confirmed by ICA, whereas >86% of the superficial calcified plaques as demonstrated on VIE were confirmed by ICA to be significant stenosis.

On a per-vessel assessment, the sensitivity, specificity, PPV, and NPV, and 95% confidence interval (CI) were 94% (95% CI: 61%, 100%), 27% (95% CI: 18%, 38%), 33% (95% CI: 23%, 43%), and 92% (95% CI: 74%, 99%) for CCTA, and 100% (95% CI: 89%, 100%), 85% (95% CI: 75%, 92%), 71% (95% CI: 56%, 84%), and 100% (95% CI: 95%, 100%) for VIE, respectively, indicating significant improvement for the assessment of coronary stenosis by VIE. Similar findings were observed at individual coronary artery assessment with high diagnostic value achieved using VIE, which is shown in Table 3. The AUC by ROC curve analysis for VIE demonstrated significant improvement for detection of >50% coronary stenosis in LAD compared with CCTA (0.99 vs 0.60, $P < 0.001$), with improved performance in LCx and RCA, although this did not reach statistical significance (0.98 vs 0.84 for LCx, 0.77 vs 0.77 for RCA, $P = 0.07$ and 0.96) (Figure 4).

Since patients in this study were scanned with different generations of multislice CT scanners, a further analysis of the

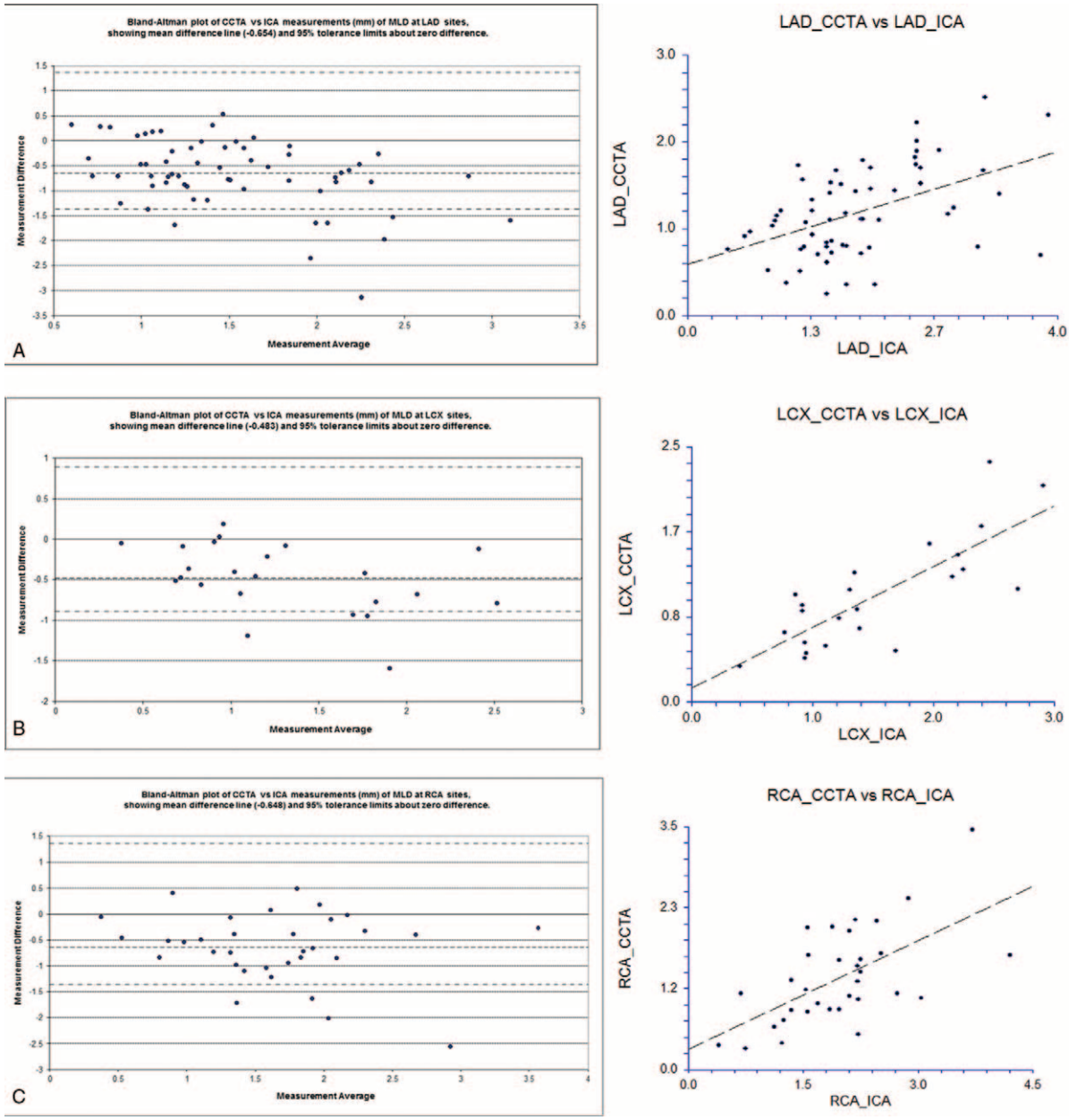

FIGURE 3. Bland–Altman plots and scatter plots with regression line of LAD, LCx, and RCA vs ICA bias, showing line of mean bias and 95% tolerance limits below zero bias (A–C). ICA = invasive coronary angiography, LAD = left anterior descending, LCx = left circumflex, RCA = right coronary artery.

diagnostic value of 64-, 128-, and 640-slice CCTA was performed to determine whether there is any significant difference between these scanners. On a per-vessel assessment, the sensitivity, specificity, PPV, and NPV, and 95% CI of CCTA and VIE in the diagnostic evaluation of CAD did not show any significant difference between these CT scanners, as shown in Table 4.

Figure 5 shows deep calcified plaques in the LAD with significant coronary stenosis on CCTA, but it was confirmed to be minimal lumen stenosis (<50%) on ICA, whereas corresponding VIE demonstrates the plaques with smooth intraluminal protrusion with no significant stenosis. Figure 6 demonstrates superficial calcified plaques in the LAD with significant coronary stenosis on CCTA, and it was confirmed to be >50% lumen stenosis on ICA, with corresponding VIE showing the plaques protruding inside the coronary lumen, resulting in significant stenosis with irregular appearances.

DISCUSSION

This study provides an insight into the relationship between calcified plaques and corresponding plaque appearances and coronary lumen stenosis in relation to the plaque features. VIE, as a novel visualization tool, may serve as a promising technique to solve the current challenge of modest diagnostic performance of CCTA, which is affected by calcified

TABLE 2. Relationship Between Calcified Plaque Types, Degree of Stenosis, and Corresponding VIE Appearances

Coronary Arteries	Plaque Distribution	Degree of Stenosis (>50%) Based on MLD by CCTA	Degree of stenosis (>50%) Based on MLD by ICA	VIE Visualization			Calcified Plaques	
				Smooth Protrusion Appearance	Protrusion, But Irregular Appearance	Degree of Stenosis (>50%)	Superficial	Deep
LAD	61	51	14	48	13	22	15	46
LCx	23	16	10	18	5	12	9	14
RCA	33	25	8	28	5	10	8	25

CCTA = coronary CT angiography, HR = heart rate, LAD = left anterior descending, LCx = left circumflex, MLD = minimal lumen diameter, RCA = right coronary artery, VIE = virtual intravascular endoscopy.

TABLE 3. Diagnostic Value of CCTA and VIE in the Detection of Coronary Stenosis When Compared With Invasive Coronary Angiography

Coronary arteries	Coronary CT Angiography								Virtual Intravascular Endoscopy							
	TP	FP	TN	FN	Sensitivity (95% CI)	Specificity (95% CI)	PPV (95% CI)	NPV (95% CI)	TP	FP	TN	FN	Sensitivity (95% CI)	Specificity (95% CI)	PPV (95% CI)	NPV (95% CI)
LAD	13	38	9	1	93% (66%, 99%)	19% (9%, 33%)	25% (14%, 39%)	90% (55%, 99%)	14	9	38	0	100% (76%, 100%)	81% (66%, 91%)	61% (38%, 80%)	100% (90%, 100%)
LCx	9	7	6	1	90% (55%, 99%)	46% (19%, 75%)	56% (30%, 82%)	86% (42%, 99%)	10	2	11	0	100% (69%, 100%)	85% (54%, 98%)	83% (51%, 98%)	100% (71%, 100%)
RCA	8	17	8	0	100% (63%, 100%)	32% (15%, 53%)	32% (15%, 53%)	100% (63%, 100%)	8	2	23	0	100% (63%, 100%)	92% (74%, 99%)	80% (44%, 98%)	100% (85%, 100%)
All 3 vessels	30	62	23	2	94% (61%, 100%)	27% (18%, 38%)	33% (23%, 43%)	92% (74%, 99%)	32	13	72	0	100% (89%, 100%)	85% (75%, 92%)	71% (56%, 84%)	100% (95%, 100%)

CCTA = coronary CT angiography, CI = confidence interval, FN = false negative, FP = false positive, LAD = left anterior descending, LCx = left circumflex, NPV = negative predictive value, PPV = positive predictive value, RCA = right coronary artery, TN = true negative, TP = true positive, VIE = virtual intravascular endoscopy.

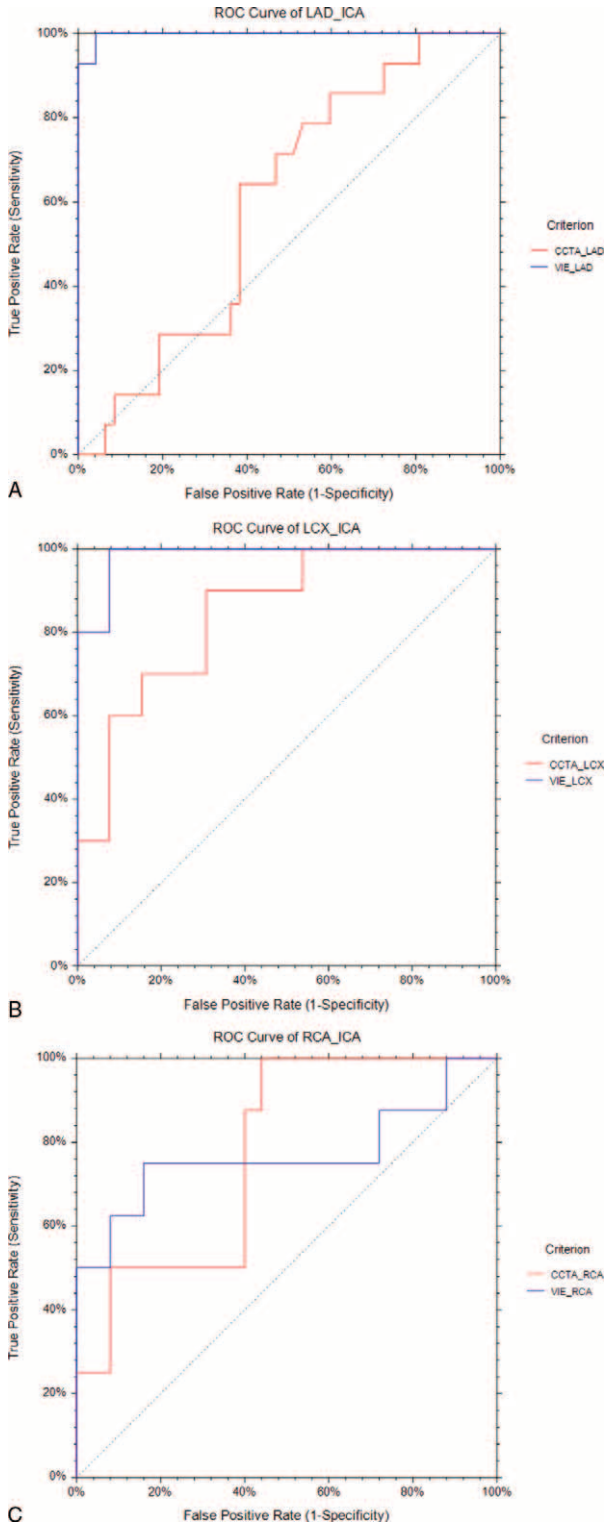

FIGURE 4. AUCs by receiver-operating characteristic curve analysis to demonstrate the diagnostic performance of VIE in the detection of coronary stenosis when compared with CCTA at LAD, LCx, and RCA (A–C). AUC = area under the curve, CCTA = coronary CT angiography, LAD = left anterior descending, LCx = left circumflex, RCA = right coronary artery, VIE = virtual intravascular endoscopy.

TABLE 4. Diagnostic Value of CCTA and VIE At Per-vessel Assessment With Use of Different Generations of Multislice CT Scanners

Type of multislice CT scanners	Sensitivity (95% CI)	Specificity (95% CI)	PPV (95% CI)	NPV (95% CI)	*P*
64-Slice CCTA	92% (61%, 99%)	27% (13%, 47%)	34% (19%, 53%)	89% (52%, 99%)	0.98
128-Slice CCTA	91% (59%, 99%)	28% (12%, 49%)	35% (19%, 56%)	88% (47%, 99%)	0.88
640-Slice CCTA	100% (73%, 100%)	26% (11%, 46%)	37% (21%, 56%)	100% (59%, 100%)	0.89
64-Slice VIE	100% (78%, 100%)	85% (65%, 95%)	78% (54%, 94%)	100% (85%, 100%)	0.98
128-Slice VIE	100% (75%, 100%)	83% (61%, 95%)	76% (50%, 93%)	100% (82%, 100%)	0.97
640-Slice VIE	100% (77%, 100%)	84% (64%, 96%)	78% (52%, 94%)	100% (84%, 100%)	0.95

CCTA = coronary CT angiography, CI = confidence interval, VIE = virtual intravascular endoscopy.

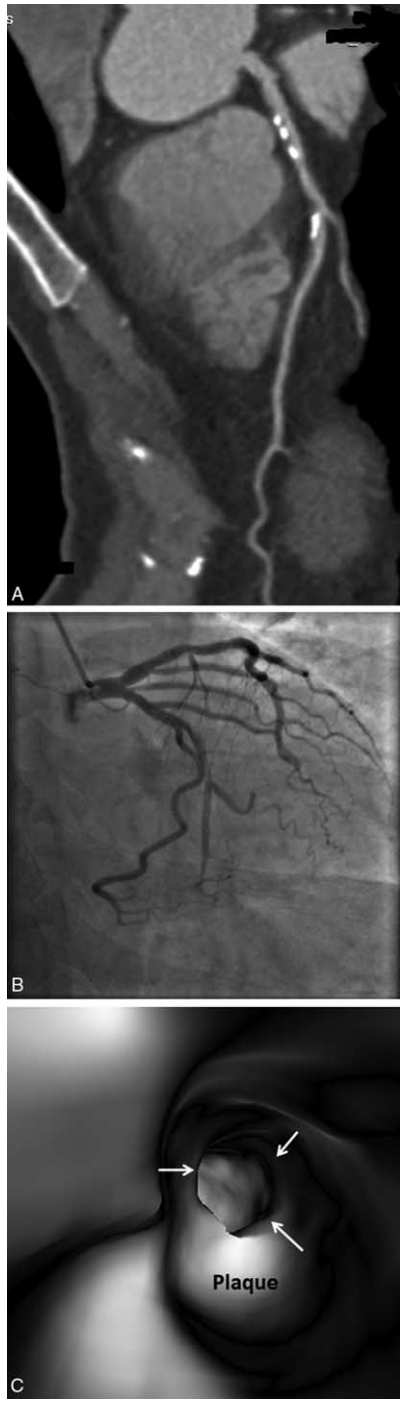

FIGURE 5. (A) Curved planar reformatted image in a 60-year-old man with suspected coronary artery disease shows calcified plaques at the proximal segment of LAD with minimal lumen diameter measured as 1.17–1.40 mm on CCTA indicating significant stenosis. (B) ICA demonstrates normal LAD with minimal lumen diameter measured as 2.82–3.37 mm. (C) VIE shows intraluminal protrusion with smooth appearance indicating that the deep calcified plaque, without causing coronary lumen stenosis. Arrows refer to the LAD intraluminal appearance on VIE. CCTA = coronary CT angiography, ICA = invasive coronary angiography, LAD = left anterior descending, LCx = left circumflex, RCA = right coronary artery, VIE = virtual intravascular endoscopy.

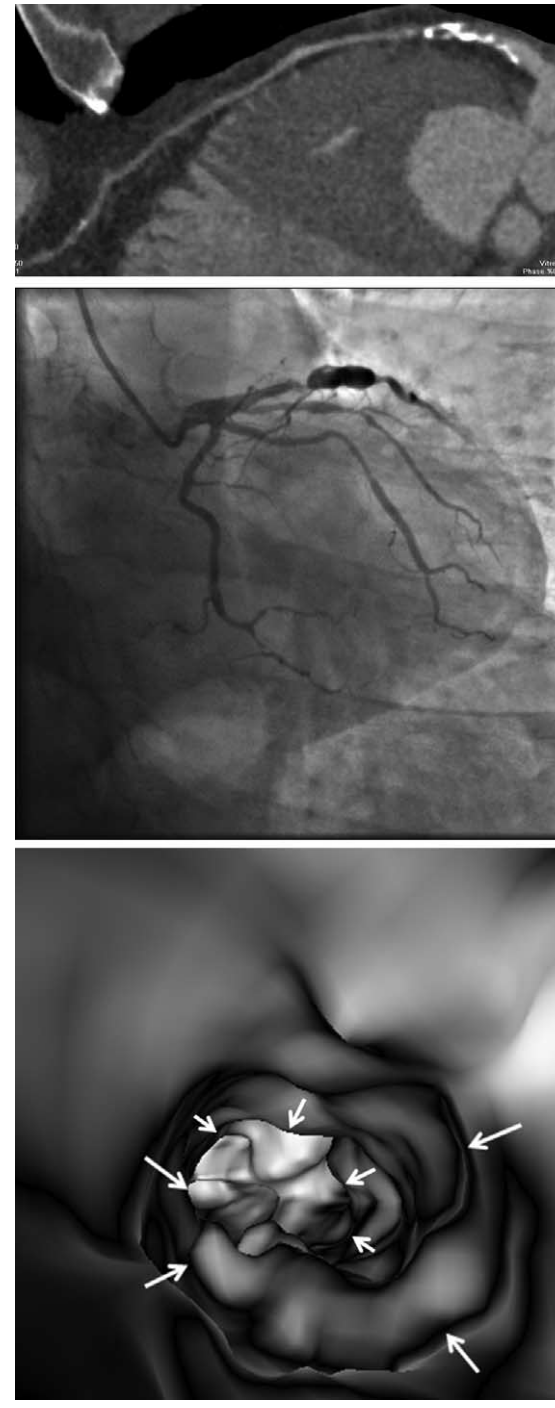

FIGURE 6. (A) Curved planar reformatted image in a 47-year-old man with suspected coronary artery disease shows calcified plaques at the proximal segment in the LAD with minimal lumen diameter measured as 0.52 mm on CCTA. (B) ICA confirmed the significant stenosis in LAD with minimal lumen diameter measured as 0.87 mm. (C) VIE demonstrates irregular intraluminal appearance in the coronary wall (long arrows) due to the superficial calcified plaque, with resultant significant stenosis. Short arrows refer to the residual LAD coronary lumen, indicating more than 50% stenosis. CCTA = coronary CT angiography, ICA = invainvasive coronary angiography, LAD = left anterior descending, VIE = virtual intravascular endoscopy.

plaques. The most important finding of this study lies in the potential value of identifying morphological features of calcified plaques in the coronary wall by VIE with significant improvement in the diagnostic value for assessment of coronary stenosis, therefore, elucidating the rationale of false positive stenosis caused by calcified plaques on CCTA.

Our findings of CCTA underestimating MLD in the presence of calcified plaques (or in other words, overestimating the degree of coronary lumen stenosis) are consistent with those reported in the literature. Results from 2 large multicenter trials showed the specificity of CCTA in patients with calcium score >400 was reduced to 20% and 53%, respectively.[7,8] Reports based on single-center experience also demonstrated negative influence of calcified plaques on the diagnostic performance of CCTA.[9–11,24] Although coronary plaques with high calcification did not significantly compromise the sensitivity and accuracy, the specificity was reduced to a greater extent in the assessment of coronary arteries with calcified plaques when compared with those with mixed or non-calcified plaques.[9–11] This is confirmed in the present study, as the specificity of CCTA is quite low ranging from 19% to 46%, whereas the sensitivity remains consistently high (≥90%) at per-vessel assessment. A recent study further verifies that the limited accuracy of CCTA in coronary lumen assessment is due to specific calcium characteristics (presence of calcium arc and mean lumen diameter).[25] The underlying mechanism may explain the fact that most of these calcified plaques belong to the deep calcified type in the coronary wall, with resultant false-positive stenosis on CCTA, but confirmed by VIE to be less significantly stenotic with improved specificity to a greater extent. On the contrary, superficial calcified plaques most commonly lead to stenosis as these plaques are close to the luminal surface area (or intima), resulting in irregular appearance as demonstrated on VIE. These findings may provide practical assistance in minimizing coronary lumen underestimation by CCTA.

Intravascular ultrasound (IVUS) is a widely used invasive imaging modality with high diagnostic accuracy for detection and quantification of CAD. IVUS allows assessment of cross-sectional vessel areas, which are closely related to hemodynamically significant coronary stenosis.[26,27] Due to its invasive nature, IVUS is not commonly performed in routine clinical practice, whereas CCTA has been increasingly used as an effective less invasive modality to diagnose CAD. CCTA has been reported to be an accurate modality for the quantitative analysis of coronary plaques, with high diagnostic sensitivity and specificity in comparison with IVUS.[28–31] Kruk et al compared CCTA and IVUS in 30 patients with regard to the vessel area assessment and CCTA ability to visualize the adventitial boarder. Their results showed high correlation between CCTA and IVUS in the evaluation of the area of external elastic membrane and adventitia ($20.2 \pm 6.4\,mm^2$ on CCTA vs $19.8 \pm 6.4\,mm^2$ on IVUS, $P < 0.001$) with a 0-HU threshold, indicating the ability of accurately delineating the adventitial border on CCTA.[32] Our results further confirm quantitative analysis of coronary plaques by CCTA from another angle with use of CCTA-generated VIE by demonstrating coronary lumen changes due to plaque features (superficial vs deep calcified plaques). Although our analysis of VIE visualization is based on a small number of cases, findings of this study have significant clinical impact because this novel visualization tool has the potential to solve the diagnostic challenge in CCTA by providing more accurate assessment of coronary stenosis, with high diagnostic performance achieved despite presence of calcified plaques.

The origin of a calcified plaque is not fully understood, but it appears to be associated with a healed fibroatheroma, whereas fibrocalcific plaques appear to be associated with a narrowed lumen due to the result of fibrosis and calcification.[14,15] IVUS has been shown to demonstrate the characteristic shape related to calcified plaques,[33] and most importantly, these calcified plaques were found to cause fewer major adverse cardiac events.[12] Calcified plaques most likely represent atherosclerotic changes at later stages of remodeling, thus reflecting more stable lesions and rarely show plaque progression.[34,35] However, the plaque in close proximity to the coronary surface (intima) may progress into luminal narrowing, followed by plaque erosion.[15] Furthermore, the pattern of calcification in plaques is also different.[36,37] Consequently, it is clinically important to characterize the calcified plaques, especially differentiation of superficial from deep plaques as the underlying mechanism for patients with higher calcification to develop future cardiac events remain to be clarified.[37,38] Optical coherence tomography (OCT) is a promising modality for in vivo identification of plaque characteristics due to its superior spatial resolution (20 μm), which allows for detection of these located on the superficial surface of plaques.[39–41] However, OCT suffers from the limited depth penetration through tissues, which is <2 mm, and this significantly affects the role of OCT to assess plaque burden. VIE has been reported as a less-invasive tool for providing detailed analysis of the calcified plaque appearances.[20–22] VIE findings in this study confirm that deep calcified plaques typically present with protrusion appearance, but with fewer cases of stenosis compared with those superficial plaques, which are found to more likely result in coronary stenosis with irregular appearances.

There are several limitations in this study. The sample size is relative small, as we only focused on analysis of calcified coronary plaques while excluding other types of plaques. This is especially apparent in the comparative analysis of LCx and RCA due to the small sample sizes of calcified plaques in these 2 arteries, which makes it difficult to detect any given difference in AUC by ROC. CCTA was performed with 64-slice CT in nearly 40% patients in this group, which could limit the diagnostic performance of CCTA in the accurate assessment of coronary stenosis when compared to 128- and 640-slice CT. Although there is no significant difference in diagnostic value between these 3 types of multislice CT scanners, further studies based on more advanced CT scanners are recommended. Calcium scoring was not available in these patients, although calcified plaques were analyzed in this study. Calcium scoring should be included as part of the CCTA examinations in future studies. Furthermore, this is a preliminary study with the proposed novel idea of using VIE to identify the calcified plaque features; however, results need to be interpreted with caution as analysis of VIE findings is based on subjective assessment with no correlation with IVUS findings. A comparison between CCTA and IVUS in a further study would allow robust conclusions to be drawn. Deep calcified plaques are shown on VIE as smooth intraluminal appearances with no significant stenosis in most of the cases; however, some of the superficial calcified plaques are also demonstrated as smooth appearances on VIE. Thus, further analysis and characterization of plaque features, in particular, analysis of those superficial plaques in relation to the development of adverse cardiac events are needed in future studies.

In conclusion, this preliminary study shows that the novel visualization tool, VIE, generated from CCTA allows for identification and analysis of calcified plaques with regard to

plaque morphology in the coronary wall, therefore, improving assessment of coronary stenosis by CCTA. A significant improvement of specificity (>80%) is achieved with use of VIE for assessment of coronary stenosis when compared with CCTA. Further studies are warranted to correlate VIE visualization with intravascular ultrasound to verify its diagnostic value in the quantitative analysis of coronary plaques.

ACKNOWLEDGMENTS

Our great appreciation is given to Mr Gil Stevenson for his assistance in the data analysis.

REFERENCES

1. Schuijf JD, Pundziute G, Jukema JW, et al. Diagnostic accuracy of 64-slice multislice computed tomography in the non-invasive evaluation of significant coronary artery disease. *Am J Cardiol.* 2006;98:145–148.
2. Vanhoenacker P, Heijenbrok-Kal M, Van Heste R, et al. Diagnostic performance of multidetector CT angiography for assessment of coronary artery disease: meta-analysis. *Radiology.* 2007;244:419–428.
3. Miller JM, Rochitte CE, Dewey M, et al. Diagnostic performance of coronary angiography by 64-row CT. *N Engl J Med.* 2008;359:2324–2336.
4. Abdulla J, Abildstrom Z, Gotzsche O, et al. 64-multislice detector computed tomography coronary angiography as potential alternative to conventional coronary angiography: a systematic review and meta-analysis. *Eur Heart J.* 2007;28:3042–3050.
5. Sun Z, Cao Y, Li HF. Multislice computed tomography angiography in the diagnosis of coronary artery disease. *J Geriatr Cardiol.* 2011;8:104–113.
6. Budoff MJ, Dowe D, Jollis JG, et al. Diagnostic performance of 64-multidetector row coronary computed tomographic angiography for evaluation of coronary artery stenosis in individuals without known coronary artery disease: results from the prospective multicenter ACCURACY (Assessment by Coronary Computed Tomographic Angiography of Individuals Undergoing Invasive Coronary Angiography) trial. *J Am Coll Cardiol.* 2008;52:1724–1732.
7. Meijboom WB, Meijs MF, Schuijf JD, et al. Diagnostic accuracy of 64-slice computed tomography coronary angiography: a prospective, multicenter, multivendor study. *J Am Coll Cardiol.* 2008;52:2135–2144.
8. Meijs MFL, Meijboom WB, Prokop M, et al. Is there a role for CT coronary angiography in patients with symptomatic angina? Effect of coronary calcium score on identification of stenosis. *Int J Cardiovasc Imaging.* 2008;25:847–854.
9. Meng L, Cui L, Cheng Y, et al. Effect of heart rate and coronary calcification on the diagnostic accuracy of the dual-source CT coronary angiography in patients with suspected coronary artery disease. *Korean J Radiol.* 2009;10:347–354.
10. Palumbo A, Maffei E, Martini C, et al. Coronary calcium score as gatekeeper for 64-slice computed tomography coronary angiography in patients with chest pain: per-segment and per-patient analysis. *Eur Radiol.* 2009;19:2127–2135.
11. Park MJ, Jung JI, Choi YS, et al. Coronary CT angiography in patients with high calcium score: evaluation of plaque characteristics and diagnostic accuracy. *Int J Cardiovasc Imaging.* 2011;27:43–51.
12. Xu Y, Mintz GS, Tam A, et al. Prevalence, distribution, predictors and outcomes of patients with calcified nodules in native coronary arteries: A 3-vessel intravascular ultrasound analysis from providing regional observations to study predictors of events in the coronary tree (PROPSECT). *Circulation.* 2012;126:537–545.
13. Sakakura K, Nakano M, Otsuka F, et al. Pathophysiology of atherosclerosis plaque progression. *Heart Lung Circ.* 2013;22:3909–4411.
14. Virmani R, Kolodgie FD, Burke AP, et al. Lessons from sudden coronary death: a comprehensive morphological classification scheme for atherosclerotic lesions. *Arterioscler Thromb Vasc Biol.* 2000;20:1262–1275.
15. Lee JB, Mintz GS, Lisauskas JB, et al. Histopathologic validation of the intravascular ultrasound diagnosis of calcified coronary artery nodules. *Am J Cardiol.* 2011;108:1547–1551.
16. Garcia-Lara J, Pinar E, Valdesuso R, et al. Percutaneous coronary intervention with rotational atherectomy for severely calcified unprotected left main: immediate and two-years follow-up results. *Catheter Cardiovasc Interv.* 2012;80:215–220.
17. Tang Z, Bai J, Su SP, et al. Cutting-balloon angioplasty for drug-eluting stent implantation for the treatment of severely calcified coronary lesions. *J Geriatr Cardiol.* 2014;11:44–49.
18. Tanigawa J, Barlis P, Di Mario C. Heavily calcified coronary lesions preclude stent apposition despite high pressure balloon dilatation and rotational atherectomy: in vivo demonstration with optical coherence tomography. *Circ J.* 2008;72:157–160.
19. Vales L, Coppola J, Kwan T. Successful expansion of an unexpanded stent by rotational atherectomy. *Int J Angiol.* 2013;1:63–68.
20. Sun Z, Dimpudus FJ, Nugroho J, et al. CT virtual intravascular endoscopy assessment of coronary artery plaques: A preliminary study. *Eur J Radiol.* 2010;75:e112–e119.
21. Sun Z. Coronary CT angiography in coronary artery disease: correlation between virtual intravascular endoscopic appearances and left bifurcation angulation and coronary plaques. *Biomed Res Int.* 2013;2013:732059.
22. Sun Z, Xu L. Coronary CT angiography in the quantitative assessment of coronary plaques. *Biomed Res Int.* 2014;2014:346380.
23. Sun Z, Winder J, Kelly B, et al. Diagnostic value of CT virtual intravascular endoscopy in aortic stent grafting. *J Endovasc Ther.* 2004;11:13–25.
24. Chen CC, Chen CC, Hsieh IC, et al. The effect of calcium score on the diagnostic accuracy of coronary computed tomography angiography. *Int J Cardiovasc Imaging.* (Suppl 1):2011:37–42.
25. Kruk M, Noll D, Achenbach S, et al. Impact of coronary artery calcium characteristics on accuracy of CT angiography. *JACC Cardiovasc Imag.* 2014;7:49–58.
26. Briguori C, Anzuini A, Airoldi F, et al. Intravascular ultrasound criteria for the assessment of the functional significance of intermediate coronary artery stenoses and comparison with fractional flow reserve. *Am J Cardiol.* 2001;87:136–141.
27. Jasti V, Ivan E, Yalamanchili V, et al. Correlations between fractional flow reserve and intravascular ultrasound in patients with an ambiguous left main coronary artery stenosis. *Circulation.* 2004;110:2831–2836.
28. Nakazato R, Shalev A, Doh JH, et al. Quantification and characterisation of coronary artery plaque volume and adverse plaque features by coronary computed tomographic angiography: a direct comparison to intravascular ultrasound. *Eur Radiol.* 2013;23:2109–2117.
29. Papadopoulou SL, Neefjes LA, Schaap M, et al. Detection and quantification of coronary atherosclerotic plaque by 64-slice multidetector CT: a systematic head-to-head comparison with intravascular ultrasound. *Atherosclerosis.* 2011;219:163–170.
30. Voros S, Rinehart S, Qian Z, et al. Prospective validation of standardized, 3-dimensional, quantitative coronary computed tomographic plaque measurements using radiofrequency backscatter intravascular ultrasound as reference standard in intermediate

coronary arterial lesions: Results from the ALTANTA (Assessment of Tissue Characteristics, Lesion Morphology, and Hemodynamics by Angiography with Fractional Flow Reserve, Intravascular Ultrasound and Virtual Histology, and Noninvasive Computed Tomography in Atherosclerotic Plaques) I Study. *JACC Cardiovasc Imaging.* 2011;4:198–205.

31. Voros S, Rinehart S, Qian Z, et al. Coronary atherosclerosis imaging by coronary CT angiography: current status, correlation with intravascular interrogation and meta-analysis. *JACC Cardiovasc Imaging*. 2011;4:537–548.
32. Kruk M, Wardziak L, Mintz GS, et al. Accuracy of coronary computed tomography angiography vs intravascular ultrasound for evaluation of vessel area. *J Cardiovasc Comput Tomogr.* 2014;8:141–148.
33. Virmani R, Burke AP, Farb A, et al. Pathology of the vulnerable plaque. *J Am Coll Cardiol.* 2006;47:C13–C18.
34. Sun Z, Choo GH, Ng KH. Coronary CT angiography: current status and continuing challenges. *Br J Radiol.* 2012;85:495–510.
35. Feng T, Yundai C, Ying Z, et al. Atherosclerotic plaque morphology indicates clinical symptoms of plaque progression. *Cardiology.* 2014;129:207–212.
36. Bentzon JF, Otsuka F, Virmani R, et al. Mechanisms of plaque formation and rupture. *Circ Res.* 2014;114:1852–1866.
37. Otsuka F, Finn AV, Virmani R. Do vulnerable and ruptured plaques hide in heavily calcified arteries? *Atherosclerosis.* 2013;229:34–37.
38. Mauriello A, Servadei F, Zoccai GB, et al. Coronary calcification identifies the vulnerable patients rather than the vulnerable plaque. *Atherosclerosis.* 2013;229:124–129.
39. Jia H, Abtahian F, Aguirre AD, et al. In vivo diagnosis of plaque erosion and calcified nodule in patients with acute coronary syndrome by intravascular optical coherence tomography. *J Am Coll Cardiol.* 2013;62:1748–1758.
40. Prati F, Regar E, Mintz GS, et al. Expert review document on methodology, terminology, and clinical applications of optical coherence tomography: physical principles, methodology of image acquisition, and clinical application for assessment of coronary arteries and atherosclerosis. *Eur Heart J.* 2010;31:401–415.
41. Raffel OC, Tearney GJ, Gauthier DD, et al. Relationship between a systemic inflammatory marker, plaque inflammation, and plaque characteristics determined by intravascular optical coherence tomography. *Arterioscler Thromb Vasc Biol.* 2007;27:1820–1827.